



## Synergistic use of sentinel-1 and sentinel-2 data for mapping of degradation in coastal forests and miombo woodlands of Tanzania

Daria C Kimaro<sup>1\*</sup>, Ernest W Mauya<sup>2</sup>, Justo N Jonas<sup>3</sup> and Charles J Kilawe<sup>3</sup>

<sup>1</sup> Department of Natural Resources Management and Conservation, Sokoine University of Agriculture, P.O. Box 82, Katavi, Tanzania

<sup>2</sup> Department of Forest Engineering and Wood Sciences, Sokoine University of Agriculture, P. O. Box 3012, Morogoro, Tanzania

<sup>3</sup> Department of Ecosystems and Conservation, Sokoine University of Agriculture, P. O. Box 3010, Morogoro, Tanzania

### Keywords

Forest degradation;  
3I3D;  
Sentinel-1;  
Sentinel-2;  
Coastal forests

### Abstract

Forest degradation is one of the leading sources of carbon emission globally. In Africa, particularly in Tanzania, forest degradation is driven by selective logging and forest fires. Monitoring degradation over large areas is very challenging due to the lack of accurate and reliable methods. This study assessed degradation in miombo woodlands and coastal forests using a synergy of remotely sensed data acquired from sentinel-1 and sentinel-2 achieved by integrating their complementary strength where sentinel-1 enhanced detection of structural changes and sentinel-2 provided spectral insight into vegetation. The 3I3D, unsupervised algorithm analysing trends for three vegetation indices (3I) in a three-dimensional feature space (3D), alongside Random Forest, Support Vector Machines to identify, classify, and map degradation indicators from July to December 2022. Results show that Random Forest had an overall accuracy of 91.6% and a Kappa statistic of 86.5%, while Support Vector Machine achieved only 58.7% accuracy. Burnt areas showed higher reflectance due to exposed soil and ash, while selective logging exhibited intermediate reflectance and radar backscatter. Non-degraded areas had lower reflectance and higher radar backscatter. Ruvu South experienced the highest disturbance with more burnt and logged areas compared to Liwale and Morogoro. Thus, demonstrating the effectiveness of the synergy of Sentinel-1 and 2 in forest degradation monitoring, providing essential insight for conservation strategies in Tanzania

### Introduction

Forests play an important role in mitigating climate change by storing carbon and accounting for one-third of CO<sub>2</sub> emitted by fossil fuel combustion by absorbing 2.4 billion metric tons of CO<sub>2</sub>. However, every year 13 million hectares of forests in the world are being destroyed through deforestation and forest degradation accounting for the release of more than 5.2GtCO<sub>2</sub>eq/yr (Bhatt 2023). Global estimations of carbon emissions from degradation range from 40% to 212% of those of deforestation and it has been rendered difficult with so many uncertainties due to it being strenuous to monitor degradation over large areas thus uncertainties remain in the role of disturbances in terrestrial carbon cycles (Gao et al. 2020). Forest degradation, as defined by the Intergovernmental Panel for Climate Change (IPCC) encompasses a long-term reduction of biological productivity, and ecological integrity, as a result of direct or indirect natural and anthropogenic factors (IPCC 2019). To address this challenge, global mechanisms such as REDD+ (Reducing Emissions from Deforestation and Forest Degradation and the role of conservation, sustainable forest management, and enhancement of forest carbon stock in developing countries) have been developed under the United Framework Convention for Climate Change (UNFCCC) (Muthee et al. 2022). These initiatives emphasize the need for robust methods for

monitoring forest disturbance, quantifying emissions, and areas lost result of disturbances.

Remote sensing has been exploited over several years in mapping and accounting for forest disturbances which leads to degradation over many years through its data (Vaglio Laurin et al. 2021). Early reliance on coarse resolution sensors such as MODIS provided higher data density and lower computational requirements, however, they had the disadvantage of missing small-scale disturbances (Tang et al. 2020). Over the past decade, advancements in medium to high-resolution satellite data have expanded the possibility of forest monitoring. The Landsat archive was made available in 2008, has since been continuously developed (Wulder et al. 2022), and the Advanced Thermal Emission and Reflection Radiometer (ASTER) was launched in 2014 (Hewson et al., 2020). In the same year, the Copernicus Programme under ESA introduced a series of satellite missions known as sentinel satellites (Phiri et al. 2020).

The sentinel 1 satellites launched in 2014 and 2016 carry dual polarized C-band SAR sensors, which provide a 12-day revisiting time at the equator, produce imagery that is not dependent on cloud cover and solar illumination thus useful for augmentation and visual interpretation (Ban et al. 2020). Radar signals emitted by sentinel-1 (S1) interact with vegetation depending on factors such as polarization, wavelength, and size of the vegetation components whereby smaller wavelengths will

\*Corresponding Author Email: [daria.kimaro@sua.ac.tz](mailto:daria.kimaro@sua.ac.tz)

Received 12 May 2025, Revised 20 May 2025, Accepted 30 May, Published December 24 2025

<https://doi.org/10.65085/2507-7961.1105>

© College of Natural and Applied Sciences, University of Dar es Salaam, 2025

ISSN 0856-1761, e-ISSN 2507-7961

interact with smaller elements such as twigs and leaves. In contrast, longer wavelength penetrates deeper and interact with branches and trunks (Balling et al. 2024). SAR emits radar signals data provide exceptional combined high spatial and temporal resolution compared to its predecessors. On the other hand, sentinel-2, a multispectral satellite imagery (MSI) launched in 2015 (Phiri et al. 2020) has a short revisiting time (5 days) providing an opportunity to acquire dense time series imagery, multiple spectral attributes, and spatial resolution bands. The sentinel-2 acquires data, including three red-edge bands which are very useful in providing information about vegetation such as chlorophyll content (Sharifi et al. 2022). sentinel-2, which consists of sentinel-2A and sentinel-2B, has a 5-day revisit period. Sentinel-2 (S2) high-resolution imagery has proven useful in mapping changes in forest and land use/land cover (LULC) (Isbaex and Margarida 2021, Phiri et al. 2020). The sentinel images have the advantage of being possible to be processed in GEE platform which has cloud computing algorithms and solves the problems related to processing large volumes of data related to large areas (Zhang et al. 2019).

The integration of these datasets on platforms like GEE further expands the potential for large-scale analysis. GEE provides access to a vast repository of geospatial datasets with planetary-scale analysis capabilities (Gorelick et al. 2017, Sidhu et al. 2018) with global applications including forest change assessment (Hansen et al. 2013). Forest disturbance detection algorithms implemented in GEE and exploiting the analysis-ready satellite data include (i) LandTrendr (Kennedy et al. 2018), (ii) Continuous Change Detection and Classification (Zhu and Woodcock 2014) (iii) Exponentially Weighted Moving Average Change Detection (Brooks et al. 2013) (iv) The Vegetation Change Tracker (Huang et al. 2010) and (v) the Verdet forest change detection algorithm (Hughes et al. 2017). All the algorithms mentioned were first designed to work with Landsat satellite imagery however some can work with imagery from different satellite emissions.

Three indices Three-dimension (3I3D) algorithm was developed in Italy and proved to be of greater consistent accuracy compared to other conventional approaches. 3I3D is an unsupervised algorithm that predicts forest changes by analysing trends for three vegetation indices (3I) used as axes of a three-dimensional feature space (3D) (Francini et al. 2022) recognized for its effectiveness in degradation and its indicators assessment and mapping. This algorithm, operating within the GEE framework, allows for the seamless integration of diverse datasets and facilitates the execution of complex degradation analyses over extensive geographical areas. The synergy between GEE's computational capabilities and advanced algorithms like 3I3D enables us to derive a comprehensive and high-resolution depiction of forest degradation patterns (Francini et al. 2022). One of the significant ways to classify degradation is using satellite

imagery using classification algorithms. These algorithms are both supervised and unsupervised, and with development, machine learning algorithms have come into existence. Vector of the MLs, Support vector machine, and random forest has become prominent and perform better compared to traditional methods. However they do not perform with the same accuracy and precision when used with different satellite imagery and therefore it is important to test and measure their performance (Avci et al. 2023).

The synergy between S1 and S2 has been used in predicting and classifying forest cover (De Luca et al. 2022, Mercier et al. 2019) and estimating and mapping aboveground biomass (Mauya et al. 2019). However, there is a lack of applying the synergy of sentinel-1 and sentinel-2 in mapping forest degradation and its indicators in the coastal forests and woodlands of Tanzania. Therefore this study intends to test and evaluate the potential of sentinel-1 and sentinel-2 in estimating and mapping forest degradation in the coastal forests and woodlands of Tanzania with the following specific objectives: i) classify and map indicators of forest degradation using sentinel-1 and sentinel-2, ii) synergy of sentinel-1 and sentinel-2 in classifying and mapping forest degradation iii) test and evaluate classification algorithms in classifying forest degradation using sentinel-1, sentinel-2 and their synergy. By integrating these datasets and methods, this study seeks to establish a comprehensive framework for efficient monitoring of forest degradation thus providing crucial insight to support REDD+ and other conservation initiatives.

## Materials and Methods

### Study area

This study was conducted in three sites namely Morogoro, Liwale, and Ruvu South Forest reserve as shown in Figure 1, allowing coverage of more forest conditions and for comparison and validation of data collected. These areas are mostly covered with woodlands and patches of coastal forests with Liwale and Morogoro dominated by woodlands while Ruvu South contains more extensive coastal forest patches. Together these sites represent a range of vegetation and human disturbances allowing evaluation of the effectiveness of satellite imageries and their synergy in mapping forest degradation. The rainfall pattern for all the sites is characterized into two: heavy rains from March to May. The short rains occur from November to January in Liwale, from October to December in Morogoro, and from September to November in Ruvu South. Vegetation groups found within the study sites include woodlands with shrubs, grasses, and tree species such as *Julbernardia globiflora*, *Brachystegia* spp., *Pterocarpus angolensis*, *Combretum* spp., grassland, cultivated land and lowland with tree species such as *Sclerocarya birrea* and *Ochna holstii*.

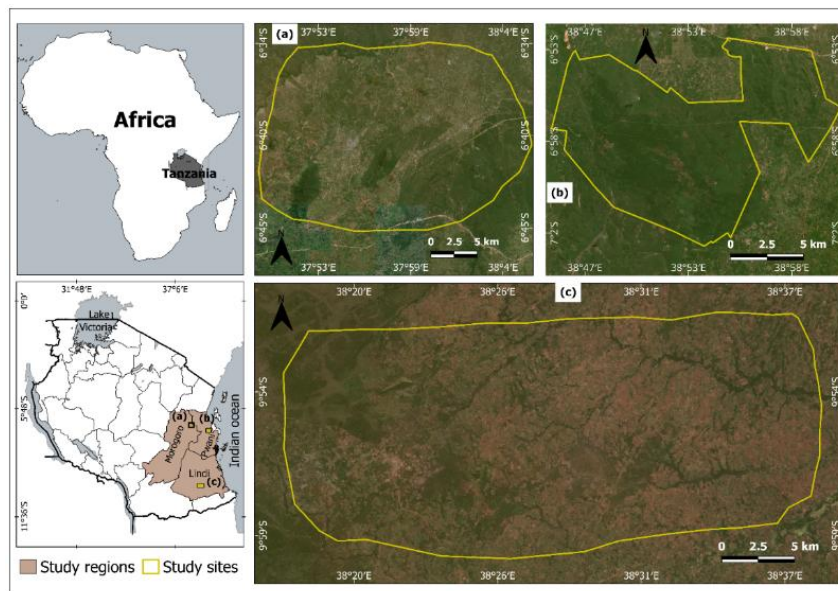


**Figure 1:** Location of the study sites in the coastal forests and woodlands of Tanzania

## Forest degradation mapping methodology

### *Sentinel-1 data*

Sentinel-1, comprising sentinel-1A and sentinel-1B, operates in the C-band with a 10m resolution and a 6-day revisit period, making it valuable for forest monitoring. This study used sentinel-1 Ground Range Detected (GRD) data from the “CORPENICUS/S1\_GRD” dataset in GEE, covering the period from July to December 2022. Images acquired were from the Interferometric Wide (IW) swath mode with descending orbit ensuring consistency in backscatter values. The analysis focused on VH polarization due to its sensitivity to vegetation structure, while VV polarization was included for additional validation. The pre-processing involved filtering by date, area of interest, and orbit direction followed by the application of a median filter for noise reduction. The change in VH backscatter was computed to highlight areas of significant vegetation loss.

### *Sentinel-2 data*

Sentinel-2 Surface Reflectance (SR) data were obtained from the “CORPENICUS/S2\_SR” dataset in GEE from July to December 2022. A total of 23 images covering the study area were used, ensuring sufficient temporal coverage and reduced atmospheric disturbances. Since optical images are affected by cloud sentinel-2 QA60 band was used for cloud and cloud shadow masking. To map and identify these indicators Cloud-free and processed sentinel-2 data were downloaded from the GEE platform. The mosaics contain Blue (B02), Green (B03), Red (B04), Red Edge 1 (B05), Red Edge 2 (B06), Red Edge 3 (B07), Near Infrared (B08), Narrow Near Infrared (B08), Shortwave Infrared 2 (B11), Short Wave Infrared 3 (B12). All the bands were then ordered at the spatial resolution of 10 m and bands with original resolution coarser than 10 m (all bands except B2-B4) were sampled to 10 m using the nearest neighbor method, as described in the S2 Global Mosaic User Manual.

## Forest Degradation and sampling

The definition may vary depending on the site, nature of degradation, or country depending on how forests are. For instance, Tanzania adopted a definition that defines forest

as an area of land with at least 0.5 ha, with a minimum tree crown cover of 10% or with existing tree species planted or natural having the potential of attaining more than 10% crown cover, and with trees which have the potential or have reached a minimum height of 3m at maturity in situ. In our study degradation is indicated by the presence and intensity of activities like selective logging and forest fires.

To monitor disturbance for the selected study period, which was 2022, three sentinel-2 images were obtained, one for the specific study year (2022), the second one for the preceding year (2021), and the last one for the subsequent year (2023). Clouds and cirrus were then masked out from the images before calculating the annual composites resulting in a cloud-free image composite for each year. The 3I3D algorithm in GEE was then applied to these composites to construct the forest disturbance maps. Three photosynthetic indices (3I) namely Normalized Burn Ratio (NBR), Normalized Difference Moisture Index (NDMI), and Moisture Stress Index (MSI) were calculated and their values were plotted in a three-dimensional (3D) space. For each pixel in satellite imagery, the algorithm analysed the values of the vegetation indices for the target year (t), the preceding year (t-1), and the subsequent year (t+1). These values were plotted within the 3D forming a point cloud representing the spectral characteristics of each pixel over the three-year period. We then manually sampled a total of 2250 training points across the three sites, whereby each was stratified into a 10km<sup>2</sup> grid whereby in each grid smaller grids of 10m by 10m were selected based on the intensity of disturbance (Fig. 2). For each cover 250 training points were selected from the image and assessed and this process was done for all the three sites making a total of 2,250 points with 70% used for training and 30% for validation (Shetty 2019, Khan et al. 2020). The training samples were selected in such a way that they were geographically scattered over the whole study area and ensured representation from each class with the same percentage of samples to avoid bias towards any class. The criteria for identifying selective logging included

canopy gaps and access roads spread across the sites, and fire areas were identified by visible burn scars of varying intensity.

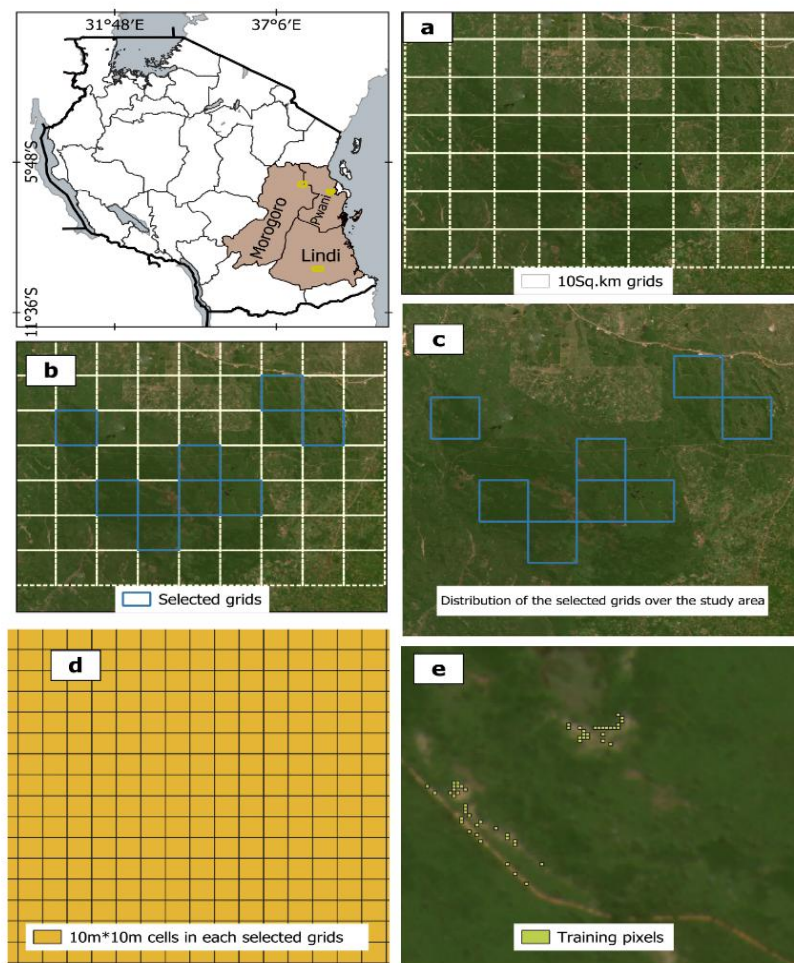


**Figure 2:** Study site location and distribution of grids (training points) within the sites

### Data analysis

The workflow of classification mapping is as shown in Figure 2. The image processing workflow for sentinel-2 MSI and sentinel-1 SAR data in GEE platform involved several key steps. Initially, the relevant satellite imagery was acquired from the GEE data catalog. Pre-processing procedures, such as radiometric calibration, atmospheric corrections for MSI, and backscatter values for SAR, were applied to ensure accurate and consistent data (Filipponi 2019). Reflectance values were then extracted from specific bands of both the sentinel-1 (SAR) and sentinel-2 (MSI) datasets for each training sample. Sentinel-1's 'VH' and 'VV' bands were chosen, as were sentinel-2's 'B2', 'B3', 'B4', 'B5', 'B6', 'B7', 'B8', 'B8A', 'B11', and 'B12'. This dual-source data extraction method ensured a thorough integration of information from radar and optical sensors. GEE provides access to machine learning algorithms such as Random Forest (RF) and Support Vector Machine (SVM) in its catalogue. These algorithms were imported into the GEE environment for use in the disturbance/degradation classification. The accuracy of the disturbance/degradation classification was assessed by comparing the classified results to the validation samples. Metrics such as producer and user

accuracy, overall accuracy, and kappa coefficient were calculated to quantify the classification performance.

### Accuracy assessment

The number of reference points collected during the field survey did not cover the entire study region (Venkatappa et al. 2019). To evaluate the performance of classification, we used 30% of the validation sample data to compare the reference labels with the predicted ones following traditional quantitative assessment methods. Conventionally, image classification and feature extract products are assessed for accuracy using an error matrix. This involves comparing classification results to a limited number of validation samples that represent mapping or assessment units, such as pixels, blocks, or image objects (Congalton 1991). Most people assume that the validation data is accurate and serve as the ground truth. Numerous metrics, such as overall accuracy (OA, Equation (1)), class-level accuracies like producer's accuracy (PA) (1–omission error) and user's accuracy (UA) (1–commission error) (Equations (2) and (3)), and the Kappa statistic (Equation (4)) can be computed by cross tabulating the classification product and related validation samples (Congalton 1991, 2001). This framework has also been used in the proposal of other measures (Maxwell & Warner, 2020). Where the Overall Accuracy (OA)

determines the algorithm's overall efficiency and is calculated by dividing the total number of correctly classified samples by the total number of tested samples. The degree of agreement between the predicted values and the ground truth data is indicated by the Kappa Statistics. Producer Accuracy (PA) calculates the accuracy of a pixel's classification. One of its components

$$\text{Overall Accuracy } O.A = \frac{\text{Number of Correctly Classified Samples}}{\text{Number of Total Samples}} \tag{1}$$

$$\text{Class Producer's Accuracy } P.A = \frac{\text{Number of Correctly Classified Samples in Category}}{\text{Number of Samples from Reference Data in Category}} \tag{2}$$

$$\text{Class User's Accuracy } U.A = \frac{\text{Number of Correctly Classified Samples in Category}}{\text{Number of Samples Classified to that Category}} \tag{3}$$

$$\text{Kappa Statistic} = \frac{\text{Overall Accuracy} - \text{Estimated Chance Agreement}}{1 - \text{Estimated Chance Agreement}} \tag{4}$$

**Results**

In mapping and classifying forest disturbances for the study sites, three (3) classes were detected that is selective logging, burnt areas and non-degraded areas using “sentinel-1”, “sentinel-2”, and a combination of both “synergies”. Figure 2 shows the reflectance of sentinel 2 bands while detecting these disturbances. A steady rise in reflectance was observed from band 5 to 8A followed by

is the error of omission, which is the percentage of ground-based features that are mistakenly removed from a class. The User Accuracy (UA) includes the error of commission, which refers to pixels that are mistakenly included in a class, and measures the map's reliability, indicating how well it depicts what is actually on the ground (Congalton 1991, Mananze et al. 2020).

a decline up to band 12 for all the classes. The highest reflectance (>3000) and lowest were observed between band 8 and 8A, B3 and B4 respectively for burnt areas from which a steady rise was observed from band 5 to band 8A and a fall in reflectance after it up to band 12 for all the classes. Highest (>3000) and lowest (<1000) reflectance were observed in burnt areas and the lowest.

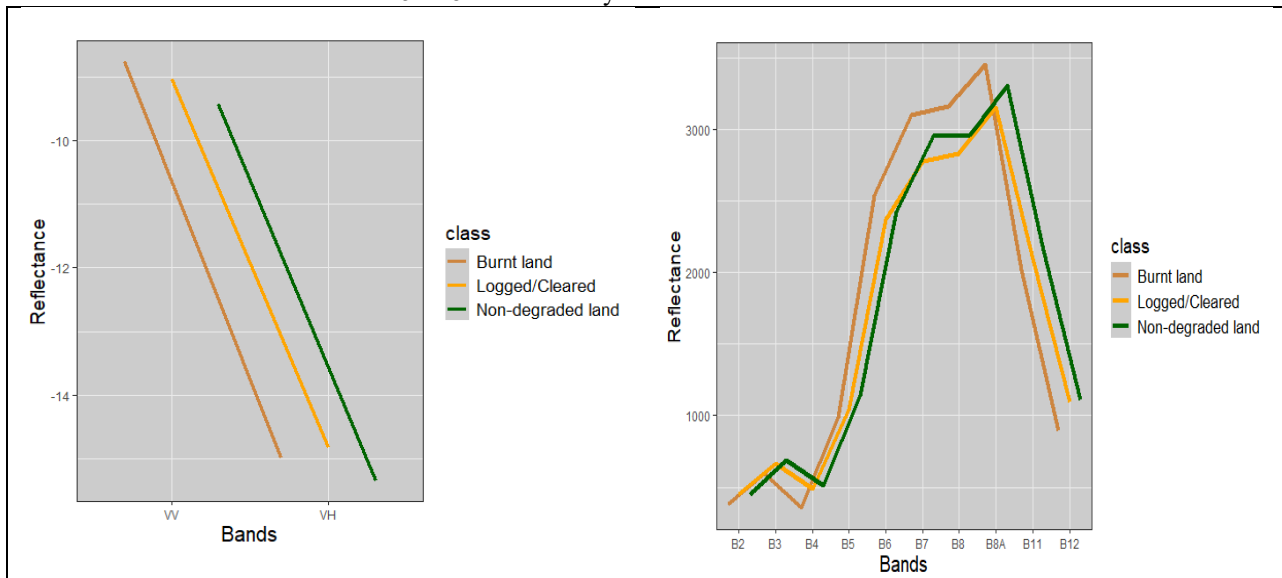


**Figure 3:** Band reflectance for sentinel-1 and sentinel-2 satellite imagery for each degradation indicator

Classification of disturbances in the study areas revealed a distinct pattern in the distribution of the disturbance classes as shown in Figure 3. Both Morogoro and Livale were dominated by non-degraded, covering over 75% of their respective landscapes, with the remaining areas classified as logged/cleared with no burnt areas detected. Ruvu South exhibited a more varied

disturbance pattern, with burnt areas accounting for approximately 25%, area coverage for burnt areas, and non-degraded areas over 50%. These findings suggest that Ruvu South has experienced more extensive disturbances compared to the other two sites.

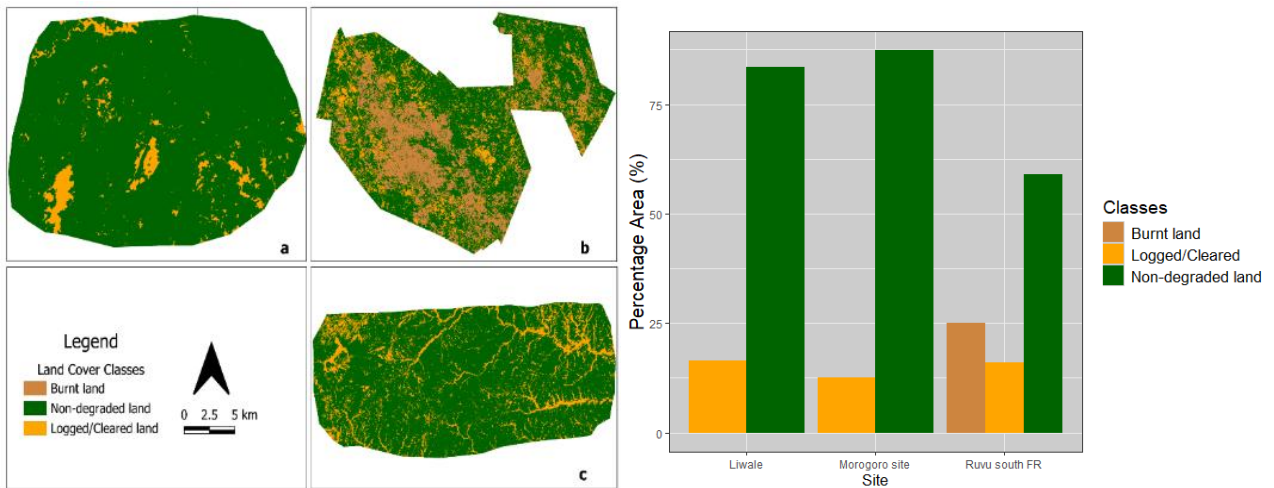


Figure 4: Degradation indicator distribution in each site

Accuracy and performance of classification algorithms for the three approaches is as shown in Table 1 and Table 2 below. For sentinel-1 RF demonstrated higher performance, achieving a producer accuracy of 97.38% for burnt areas compared to SVM's lowest accuracy of 58.1% reflecting RF's ability to reduce omission errors and detect fire-affected areas effectively. In case of sentinel-2 highest P.A was observed while classifying non-degraded areas using SVM and lowest in selective logging. Highest (85.71%) and lowest (64.71%) were observed in burnt areas and non-degraded land respectively while using RF for classification. When

sentinel-1 was used alone, RF achieved an overall accuracy of 83.23% significantly outperforming SVM's 45.24%, highlighting RF's ability to handle radar data effectively. The combined detection (S1 and S2 synergy) showed higher degree of agreement and effectiveness of algorithms for RF (86.49%) compared to SVM (31.08%) with an overall accuracy of 91.62% and 58.68% respectively suggesting that synergy map results are highly complementary and indicate SVM's limitation in handling complex data.

Table 1: Performance of machine learning algorithms for disturbance mapping based on sentinel-1 and 2 independent data.

Disturbance classes	Sentinel-1				Sentinel-2			
	RF		SVM		RF		SVM	
	U.A %	P.A %	U.A %	P.A %	U.A %	P.A %	U.A %	P.A %
Non-degraded	67.79	86.95	58.3	77.7	64.71	61.11	75.00	83.30
Selective cutting	91.18	74.70	58.800	60.6	68.18	77.00	75.00	50.00
Burnt areas	92.50	97.39	58.10	58.1	85.71	80.00	76.92	73.33
<b>Overall accuracy (%)</b>	83.23		58.20		71.69		67.62	
<b>Kappa statistics (%)</b>	74.03		45.24		57.10		52.30	

Table 2: Performance of machine learning algorithms for degradation mapping based on sentinel-1 and 2 synergies

Disturbance classes	Sentinel-1 and 2			
	RF		SVM	
	U. A %	P. A %	U. A %	P. A %
Non-degraded	94.87	80.43	55.17	34.78
Selective logging	89.66	93.98	62.75	77.11
Burnt area	92.68	100	50.00	47.37
<b>Overall accuracy (%)</b>	<b>91.62</b>		<b>58.68</b>	
<b>Kappa statistics (%)</b>	<b>86.50</b>		<b>31.09</b>	

**Discussion**

The study's main objective was to test the performance of sentinel-1 and sentinel-2 in estimating and mapping forest degradation in the coastal forests and woodlands of Tanzania, which are highly vulnerable to anthropogenic

pressures. In recent years Tanzania has been facing a major increase in degradation activities and thus making the use of satellite imagery and their synergy becomes crucial in covering areas that cannot be covered by field inventory data.

In this study, we showed how multispectral (sentinel-2) and SAR (sentinel-1), their synergy and classification algorithms can give promising results by assessing their accuracy and performance and selecting the best to obtain a detailed forest degradation map. Overall, our study has shown that synergy of the two-satellite imagery has better performance in estimating and mapping forest degradation and its indicators. With sentinel-2 imagery a sharp increase in reflectance in the near-infrared (NIR) region was observed, particularly between bands 8 and 8A, which is most pronounced in burnt areas, and can be attributed to the structural damage caused by fire. Fire reduces the chlorophyll content and increases soil exposure, leading to higher reflectance in the NIR bands which are sensitive to total chlorophyll, biomass, leaf area index (LAI), and water absorption reference (Misra et al. 2020). Such case was the same as studies done by (Chuvieco et al. 2019) and (Ramo et al. 2021) who reported that burnt areas exhibit high NIR reflectance due to the loss of vegetation cover and the presence of ash and charred material. Our study also reflects the varying degrees of forest disturbance, with lower reflectance in these bands for burnt and selectively logged areas compared to non-degraded forests. Band 2, sensitive to senescence, carotenoids, and browning of vegetation (Misra et al. 2020), shows lower reflectance in burnt areas due to the loss of healthy vegetation and increased browning from fire damage. Band 3, which is sensitive to total chlorophyll content, also exhibits lower reflectance in disturbed areas because of reduced chlorophyll levels following logging or burning. Similarly, band 4, where maximum chlorophyll absorption occurs, shows the lowest reflectance in non-degraded areas with healthy vegetation, while disturbed areas have reduced absorption due to the loss of photosynthetic activity.

The differences in radar reflectance observed between the degradation indicators provide insight into how degraded and non-degraded areas respond to radar signals. Lower reflectance in the VH band across all indicators likely reflect the fact that VH polarization is more sensitive to vegetation structure and biomass, resulting in lower backscatter in burnt areas due to reduction in structural components that scatter radar signals. Logged/cleared areas, while still degraded, showed higher reflectance than burnt areas suggesting that some vegetation remain in logged areas allowing a slightly stronger radar return. The higher reflectance in nondegraded areas reflects the presence of intact vegetation contributing to greater radar backscatter.

In burnt areas, the radar backscatter was markedly reduced, which can be attributed to loss of structural vegetation components like leaves, branches, and smaller plants, all of which play a role in scattering radar signals (Mutai 2019). When fire damages or destroy these elements, the ability of the landscape to scatter signals reduces leading to lower backscatter (Tanase et al. 2010). This reduction is particularly evident in the VH band, where polarization is better suited to capturing horizontal scattering. In logged/cleared areas, while degradation is evident, the radar reflectance was higher than that of burnt areas suggesting that some vegetation, such as smaller trees or remnant canopy, remains after logging allowing for stronger backscatter. SAR is particularly effective in

identifying this type of degradation because the difference in backscatter between areas that are partially cleared and those that are burnt is detectable (De Luca et al. 2021). Non-degraded areas, on the other hand, exhibited highest radar reflectance, reflecting the presence of fully intact vegetated forest, which is expected to have high biomass thus generating more substantial radar backscatters because of increased number of structural components such as leaves and branches. This strong radar return from non-degraded areas indicate a healthy forest structure with a high level of complexity, both horizontally and vertically, which is consistent with the behavior of undisturbed forest (Hansen et al. 2020).

The synergy between sentinel-1 and sentinel-2 significantly improved classification accuracy in this study, particularly when RF was used, a finding supported by (Cherian 2024). The integration of radar (sentinel-1) and optical (sentinel-2) data have proved to be highly effective for monitoring forest degradation, offering the advantage of combining complementary information. Sentinel-1 SAR data captures structural attributes such as biomass, canopy height, while sentinel-2 optical data provides detailed spectral information which is sensitive to vegetation health, canopy cover and leaf pigmentation (De Luca et al. 2022, Mngadi et al. 2021). By combining these datasets, forest degradation detection is improved and changes missed when either one is used alone are covered. The increase in overall accuracy in this study underscores the value of integrating radar and optical datasets for forest degradation monitoring. (Heckel et al. 2020) also supports synergy of these datasets by suggesting that they capture both structural and spectral changes in forests, thus complimenting each other in detecting forest degradation. Jiang et al. (2022) also reports similar improvements in China when combining SAR and optical data. This study found that the fusion of these datasets led to a significant enhancement in distinguishing forest and non-forested areas, an improved forest change detecting when synergy of the data set was used in China. Furthermore, the results also strongly suggest that RF is a superior classifier compared to SVM especially when synergy of datasets is used. The improved accuracy across all classes/indicators with RF highlights its ability and effectiveness in capturing both spectral and structural features. RF, as a machine learning algorithm, works by constructing multiple decision trees and aggregating their predictions which makes it highly effective for handling complexity and variability in forest degradation data. In contrast, while SVM is a powerful classifier, its performance usually depends on the complexity of the datasets. For this case, RF outperform SVM due to its robustness to overfitting and its ability to handle large volumes of data. These findings are consistent with (Cherian 2024) in India, where it was noted that RF strength lies in its flexibility and capability to capture interaction between spectral bands, radar backscatter and forest structure. Shen et al. (2023) also found that RF outperforms SVM in a study on forest degradation in Asia where the synergy boosted classification accuracy.

From the best classifier, that is RF maps were produced to show the distribution and coverage of the indicators in all the study sites where a distinct spatial pattern and

degree of degradation was depicted. In contrast to Liwale and Morogoro, Ruvu South presented a more disturbed landscape with a higher proportion of burnt areas and logged areas likely driven by charcoal making. The impact of fire on tropical forests is significant as it alters species composition, reducing biomass making the areas more vulnerable to further degradation. The indicators in Ruvu South also reflect extensive human activities influenced by its proximity to urban centers, particularly Dar es Salaam, where high population density drives greater demand for fuelwood and timber (Gwegime et al. 2013).

The findings of this study underscore the critical importance of using remote sensing technologies, specifically the synergy of sentinel-1 and sentinel-2 datasets, to monitor forest degradation. As degradation increases across Tanzania, particularly in regions close to urban centers like Ruvu South, the ability to detect and classify degraded areas accurately becomes ever more essential. The clear distinction between degradation indicators—non-degraded, logged/cleared, and burnt—demonstrates the effectiveness of combining SAR and optical imagery. Additionally, the superior performance of the RF classifier further enhances the ability to capture both structural and spectral changes in the landscape. Future research could explore deep learning algorithms such as Convolutional Neural Networks (CNNs), to further enhance classification accuracy. Additionally, leveraging synergy with other satellite imagery such as planetscope, or upcoming missions like NISAR, could improve monitoring capabilities. Expanding the use of advanced cloud computing and automated detection systems would allow for more cost-effective, scalable monitoring efforts, supporting REDD+ initiatives and better forest management practices.

## Conclusion

In conclusion, this study highlights the value of integrating SAR and MSI datasets for mapping forest degradation, offering a more accurate and comprehensive understanding of degradation indicators, with Random Forest improving classification accuracy and providing reliable tool for forest monitoring. While sentinel-1 had limited sensitivity to subtle canopy changes, and sentinel-2 from cloud cover and oversaturation, these drawbacks were mitigated through sensor integration, feature selection and use of machine learning algorithms, which together improved classification performance. offers than either method alone. Further research could address these limitations by integrating higher resolution or complimentary datasets such as LiDAR and TanDEM-X to capture finer structural and spectral details alongside advanced deep learning approaches to enhance monitoring across diverse forest ecosystems.

## Acknowledgments

The authors would like to thank Tanzania Forest Fund (TaFF) for their contribution in funding the research.

## Conflict of interest

The authors declare no conflict of interest

## References

- Avcı C, Budak M, Yağmur N, and Balçık F 2023 Comparison between random forest and support vector machine algorithms for LULC classification. *Int. J. Eng. Geosci.* 8(1): 1–10.
- Balling J., Slagter B., van der Woude S, Herold M, and Reiche J 2024. ALOS-2 PALSAR-2 ScanSAR and Sentinel-1 data for timely tropical forest disturbance mapping: A case study for Sumatra, Indonesia. *Int. J. Appl. Earth Observ. Geoinform.* 132: 103994.
- Ban Y, Zhang P, Nascetti A, Bevington AR, and Wulder MA 2020 Near real-time wildfire progression monitoring with Sentinel-1 SAR time series and deep learning. *Sci. Rep.* 10(1): 1322.
- Bhatt RP 2023 Achievement of SDGS globally in biodiversity conservation and reduction of greenhouse gas emissions by using green energy and maintaining forest cover. *GSC Adv. Res. Rev.* 17(3): 001–021.
- Brooks EB, Wynne, RH, Thomas VA, Blinn CE, and Coulston JW 2013 On-the-fly massively multitemporal change detection using statistical quality control charts and Landsat data. *IEEE Trans. Geosci. Remote Sens.* 52(6): 3316–3332.
- Cherian SM, and KR 2024 Random forest and support vector machine classifiers for coastal wetland characterization using the combination of features derived from optical data and synthetic aperture radar dataset. *J. Water Climate Change*: 15(1): 29–49.
- Chuvieco E, Mouillot F, Van der Werf GR, San Miguel J, Tanase
- M, Koutsias N., García M, Yebra M, Padilla M, and Gitas I 2019 Historical background and current developments for mapping burned area from satellite Earth observation. *Remote Sens. Environ.* 225: 45–64.
- Congalton RG 1991 A review of assessing the accuracy of classifications of remotely sensed data. *Remote Sens. Environ.* 37(1): 35–46.
- Congalton RG 2001 Accuracy assessment and validation of remotely sensed and other spatial information. *Int. J. Wildland Fire.* 10(4): 321–328.
- De Luca G, MN Silva J, Di Fazio S, and Modica G 2022 Integrated use of Sentinel-1 and Sentinel-2 data and open-source machine learning algorithms for land cover mapping in a Mediterranean region. *Eur. J. Remote Sens.* 55(1) : 52–70.
- De Luca G, Silva JM, and Modica G 2021 A workflow based on Sentinel-1 SAR data and open-source algorithms for unsupervised burned area detection in Mediterranean ecosystems. *GI Sci. Remote Sens.* 58(4), 516–541.
- Francini S, McRoberts RE, D’Amico G, Coops NC, Hermosilla T, White JC, Wulder MA, Marchetti M, Mugnozza GS, and Chirici G 2022 An open science and open data approach for the statistically robust estimation of forest disturbance areas. *Int. J. Appl. Earth Observ. Geoinform.* 106: 102663.
- Gao Y, Skutsch M, Paneque-Gálvez J, and Ghilardi A 2020 Remote sensing of forest degradation: A review. *Environ. Res. Lett.* 15(10): 103001.
- Gorelick N, Hancher M, Dixon M, Ilyushchenko S, Thau D, and Moore R 2017 Google Earth Engine: Planetary-scale geospatial analysis for everyone. *Remote Sens. Environ.* 202: 18–27.

- Gwegime J, Mwangoka M, Mulungu E, Perkin A, and Nowak K 2013. The biodiversity and forest condition of Ruvu South Forest Reserve. *TFCG Tech. Paper*: 37(2023).
- Hansen JN, Mitchard, ET, and King S 2020 Assessing forest/non-forest separability using Sentinel-1 c-band synthetic aperture radar. *Remote Sens.* 12(11): 1899.
- Hansen MC, Potapov PV, Moore R, Hancher M, Turubanova SA, Tyukavina A, Thau D, Stehman SV, Goetz SJ, and Loveland TR 2013 High-resolution global maps of 21st-century forest cover change. *Science* 342(6160): 850–853.
- Heckel K, Urban M, Schratz, P, Mahecha MD, and Schmillius C 2020 Predicting forest cover in distinct ecosystems: The potential of multi-source Sentinel-1 and-2 data fusion. *Remote Sens.* 12(2): 302.
- Hewson R, Mshiu E., Hecker C, van der Werff, H, van Ruitenbeek F, Alkema D, and van der Meer F 2020 The application of day and night time ASTER satellite imagery for geothermal and mineral mapping in East Africa. *International Journal of Applied Earth Observation and Geoinformation.* 85: 101991.
- Huang C, Goward SN, Mask JG, Thomas N, Zhu Z, and Vogelmann, JE 2010. An automated approach for reconstructing recent forest disturbance history using dense Landsat time series stacks. *Remote Sens. Environ.* 114(1): 183–198.
- Hughes MJ, Kaylor, SD, and Hayes DJ 2017 Patch-based forest change detection from Landsat time series. *Forests.* 8(5): 166.
- IPCC 2019 *Climate change and land: An IPCC special report on climate change, desertification, land degradation, sustainable land management, food security, and greenhouse gas fluxes in terrestrial ecosystems* (Eds. V. Masson-Delmotte PR, Shukla J, Skea E, Calvo Buendia HO, Pörtner DC, Roberts P, Zhai R, Slade S, Connors R, and Van Diemen).
- Isbaex C, and Margarida CA 2021 *The Potential of Sentinel-2 Satellite Images for Land-Cover/Land-Use and Forest Biomass Estimation: A Review.* Forest Biomass-From Trees to Energy, IntechOpen.
- Jiang J, Xing Y, Wei W, Yan E, Xiang J, and Mo D 2022 DSNUNet: An improved forest change detection network by combining sentinel-1 and sentinel-2 images. *Remote Sens.* 14(19): 5046.
- Kennedy RE, Yang Z, Gorelick N, Braaten J, Cavalcante L, Cohen WB, and Healey S 2018 Implementation of the LandTrendr algorithm on google earth engine. *Remote Sens.* 10(5): 691.
- Khan AA, Jamil A, Hussain D, Taj M, Jabeen G, and Malik MK 2020. Machine-learning algorithms for mapping debris-covered glaciers: The Hunza Basin case study. *Ieee Access* 8: 12725–12734.
- Mananze S, Pôças I, and Cunha M 2020 Mapping and assessing the dynamics of shifting agricultural landscapes using google earth engine cloud computing, a case study in Mozambique. *Remote Sens.* 12(8): 1279.
- Mauya EW, Koskinen J, Tegel K, Hämäläinen J., Kauranne T, and Käyhkö N 2019 Modelling and predicting the growing stock volume in small-scale plantation forests of Tanzania using multi-sensor image synergy. *Forests.* 10(3): 279.
- Mercier A, Betbeder J, Rumiano F, Baudry J, Gond V, Blanc L, Bourgoïn C, Cornu G, Ciudad C, and Marchamalo M 2019 Evaluation of Sentinel-1 and 2 time series for land cover classification of forest–agriculture mosaics in temperate and tropical landscapes. *Remote Sens.* 11(8): 979.
- Misra, G, Cawkwell F, and Wingler A 2020 Status of phenological research using Sentinel-2 data: A review. *Remote Sens.* 12(17): 2760.
- Mngadi M, Odindi J, Peerbhay K, and Mutanga O 2021 Examining the effectiveness of Sentinel-1 and 2 imagery for commercial forest species mapping. *Geocarto Int.* 36(1): 1–12.
- Mutai SC 2019 *Analysis of burnt scar using optical and radar satellite data*, Master's thesis, University of Twente.
- Muthee K, Duguma L, Wainaina P, Minang P, and Nzyoka J 2022 A review of global policy mechanisms designed for tropical forests conservation and climate risks management. *Front. Forests Global Change.* 4: 748170.
- Phiri D, Simwanda M, Salekin S, Nyirenda VR, Murayama Y, and Ranagalage M 2020 Sentinel-2 data for land cover/use mapping: A review. *Remote Sens.* 12(14): 2291.
- Ramo R, Roteta E, Bistinas I, Van Wees D, Bastarrika, A, Chuvieco E, and Van der Werf, GR 2021 African burned area and fire carbon emissions are strongly impacted by small fires undetected by coarse resolution satellite data. *Proc. Nat. Acad. Sci.* 118(9): e2011160118.
- Sharifi A, Felegari, S, and Tariq A 2022 Mangrove forests mapping using Sentinel-1 and Sentinel-2 satellite images. *Arabian J. Geosci.* 15(20): 1593.
- Shen Z, Miao J, Wang J, Zhao D, Tang A, and Zhen J 2023 Evaluating Feature Selection Methods and Machine Learning Algorithms for Mapping Mangrove Forests Using Optical and Synthetic Aperture Radar Data. *Remote Sens.* 15(23): 5621.
- Shetty S 2019 *Analysis of machine learning classifiers for LULC classification on Google Earth Engine.* M Sc. thesis, University of Twente.
- Sidhu N, Pebesma, E, and Câmara G 2018 Using Google Earth Engine to detect land cover change: Singapore as a use case. *Eur. J. Remote Sens.* 51(1): 486–500.
- Tanase MA., Santoro M, de La Riva J, Fernando P, and Le Toan T 2010 Sensitivity of X-, C-, and L-band SAR backscatter to burn severity in Mediterranean pine forests. *IEEE Trans. Geosci. Remote Sens.* 48(10): 3663–3675.
- Tang X, Bullock EL, Olofsson P, and Woodcock CE 2020 Can VIIRS continue the legacy of MODIS for near real-time monitoring of tropical forest disturbance? *Remote Sens. Environ.* 249: 112024.
- Vaglio LG, Francini S, Luti T, Chirici G, Pirotti F, and Papale D 2021 Satellite open data to monitor forest damage caused by extreme climate-induced events: A case study of the Vaia storm in Northern Italy. *Forestry* 94(3): 407–416.
- Wulder MA, Roy DP, Radeloff VC, Loveland TR., Anderson MC, Johnson DM, Healey S, Zhu Z, Scambos TA, and Pahlevan N 2022 Fifty years of Landsat science and impacts. *Remote Sens. Environ.* 280: 113195.

Zhang W, Brandt M, Wang Q, Prishchepov AV, Tucker CJ, Li Y, Lyu H, and Fensholt R 2019 From woody cover to woody canopies: How Sentinel-1 and Sentinel-2 data advance the mapping of woody plants in savannas. *Remote Sens. Environ.* 234: 111465.

Zhu Z, and Woodcock CE 2014 Continuous change detection and classification of land cover using all available Landsat data. *Remote Sens. Environ.* 144: 152–171.